

Influence of the Planetary Boundary Layer Physics on Medium-range Prediction of Monsoon over India

SWATI BASU,¹ SETHU RAMAN,² U. C. MOHANTY³ and E. N. RAJAGOPAL¹

Abstract—The present study emphasizes the importance of proper representation of boundary layer physics in a general circulation model. The Turbulent Kinetic Energy (TKE) closure scheme incorporates important processes of the Planetary Boundary Layer (PBL) compared to a simplistic first-order closure model. Hence the model which has the TKE closure scheme is capable of simulating important weather systems associated with summer monsoon, such as monsoon depressions and lows that form over the Indian subcontinent quite well compared to the first-order closure model. The present study indicates better performance of the global model with the TKE scheme in the prediction of the monsoon circulation, including the tracks of the depressions over the Indian subcontinent. Medium-range weather prediction has also improved with the use of the TKE closure. However further studies are necessary to improve the forecast, with emphasis on boundary layer processes.

Key words: PBL parameterisation, TKE closure, Indian summer monsoon, monsoon depression, medium-range forecast.

1. Introduction

The Indian summer monsoon season is the principal rainy season for India which significantly influences the agricultural sector of the country. The Arabian Sea, the Bay of Bengal and the Indian Ocean act as main reservoirs of heat and moisture in supplying the necessary energy to maintain the large-scale monsoon circulation and associated weather phenomena over the Indian subcontinent. Observations indicate (ASNANI, 1993) that during the summer monsoons there is a significant inflow of moisture from the south in the region of 0°N–30°N. The latent heat of water vapour that is set free in the moist southwest current over land leads to the enhancement of convective currents and cloud growth.

¹ National Centre for Medium Range Weather Forecasting, Mausam Bhavan Complex, Lodi Road, New Delhi-110003, India.

² Department of Marine, Earth and Atmospheric Sciences, North Carolina State University, Raleigh, North Carolina 27695-8208, U.S.A.

³ Centre for Atmospheric Sciences, Indian Institute of Technology, Hauz Khas, New Delhi-110016, India.

The rate at which water vapour is injected into the free atmosphere depends on the properties of the Planetary Boundary Layer (PBL). Over the tropics, diurnal variation of meteorological parameters within the PBL is large as compared to the extratropical region. This causes significant diurnal oscillation in wind speed, static instabilities, turbulent exchanges and convective activity (ASNANI, 1993). In addition to the transport and diffusion mechanisms of various meteorological parameters, frictional convergence takes place within the PBL. In the tropics, it is of added importance because of its role in maintaining deep convection. Air masses become considerably modified through surface exchange processes in the PBL. The structure of the PBL over the Arabian Sea is unique, compared to those over the extratropical oceans, due to the presence of a pronounced temperature inversion (PANT, 1993). This is particularly important over the western Arabian Sea where the inversion height is less (RAO and AKSKAL, 1994). The low-level Somali jet strongly influences the commencement of the monsoon over India, and it owes its existence to the unique structure of the PBL over the Arabian Sea. Further, the southwest monsoon is associated with a semi-permanent low-pressure region extending from NW India to SE India, known as the monsoon trough. This trough line runs approximately through 29°N, 77°E to 23°N, 88°E through 26°N, 82°E. This is merely a line of symmetry between the westerlies or south westerlies to its south and easterlies or south easterlies to its north. An extension of this axis in the Bay of Bengal is often a precursor of a Bay of Bengal depression. Because of the trough and the convergence in it, it is a cyclogenetic region. This trough line is a characteristic feature that is confined to the troposphere within 700 hPa. Hence, it becomes important, that for any effective prediction of the monsoon systems over the Indian subcontinent the boundary layer structure should be represented well.

The main rain-bearing systems over central and northern India are the passage of lows and depressions along the semi-permanent monsoon trough over the Indian subcontinent. The monsoon depressions are the low-pressure weather systems with two or three closed isobars (at 2 hPa intervals) which cover an area of about 5 degrees square (RAO, 1976). They are referred to as depressions when surface winds reach 33 knots (while over sea) and tropical storms when higher speeds prevail. Weaker systems with one closed isobar are called lows. They usually form over the Bay of Bengal and the Arabian Sea and move inland and subsequently dissipate.

Based on 100 years of data (1877–1976) it was found (MOHANTY, 1994) that the maximum number of cyclonic disturbances (about 60% of the annual) occurs during the southwest monsoon months (June–September). The genesis of these systems is mainly over the northern sector of the Bay of Bengal. It is interesting to note that though the maximum number of cyclonic disturbances are formed during the summer monsoon season, only about 7% of these intensify into tropical storms or severe tropical storms (MOHANTY, 1994). Furthermore, these depressions form over land as well (about 10%). On the average one depression develops over land in a year during the monsoon season. Another interesting aspect of the monsoon

depressions is that they move along the monsoon trough over north India with slight decrease in intensity, and in certain cases even intensify as they move towards the northwest sector of India. It is found that a strong low-level wind (at about 850 hPa) with substantial moisture fluxes from the Arabian Sea and the Bay of Bengal assists monsoon depressions to remain active during the passage over land parallel to the monsoon trough axis. Another factor could be the surface soil moisture gradients which contribute to sensible heat flux gradients (RAMAN *et al.*, 1988).

It is important that the various features of the monsoon circulation as well as the formation and movement of the lows and depressions are simulated well with the numerical models in order to predict the rainfall over India with reasonable accuracy. In this paper, an attempt is made to examine the medium range (3–5 days) simulation of monsoon circulation over India with a general circulation model, and the influence of the planetary boundary layer parameterization on such simulations.

2. Model Description

The National Center for Medium Range Weather Forecasting (NCMRWF) model is an adapted version of the NCEP (National Center for Environment Prediction) 18 layer global spectral model with a terrain-following coordinate. It has a spectral horizontal representation of triangular truncation at wave number 80. The main prognostic variables of the model are relative vorticity, divergence, virtual temperature, surface pressure and specific humidity. A semi-implicit time integration scheme with a 15-minute time step is utilized. At the sea surface, climatological SSTs (Sea Surface Temperature) are used and kept constant during the integration of the model extending to five days. Over land, ground temperature and soil wetness are predicted, based on energy balance and water budget at the surface. The global data assimilation scheme involves the Spectral Statistical Interpolation (SSI) and six-hour forecasts, with climatological surface values providing the first estimate for the subsequent analysis. Five-day forecasts are obtained on real time, based on the analysis at 00 UTC. Three soil layers are defined at depths of 10, 50 and 500 cm, respectively. Temperature at 500 cm is kept fixed while the soil temperature at other levels is predicted. The PBL has two layers, the surface layer, for which the Monin Obukhov similarity theory is used, and the mixed layer where the eddy transport takes place through Richardson number dependent vertical diffusion processes. The modified Kuo scheme is used for deep convection and ANTHES (1977) and TIEDKE's (1983) schemes are used for shallow convection. The LACIS and HANSEN scheme (1974) is used for short-wave radiation and FELS and SCHWARZKOPF's (1975) for long-wave radiation. This latter scheme also considers the effects of water vapour, carbon dioxide, ozone and clouds. The cloud schemes in the model are by SLINGO (1987). A summary of the

main features of the operational model is given in Table 1. The details of the forecast model and assimilation system of the NCEP are given in KANAMITSU (1989) and PARRISH and DERBER (1992).

3. Analysis—Forecast System and the Numerical Experiments

The medium-range Analysis Forecast System (MAFS) of the NCMRWF consists of data processing and quality control, data assimilation, model integration, post-processing, diagnostics and preparation of location specific agro-meteorological forecasts. Various surface and upper layer data received from the GTS with ± 3 hours of the analysis time are utilised in a six hourly assimilation cycle (Fig. 1). The analysis at 00 UTC is utilised for obtaining 5-day forecasts in real time. Synoptic conditions are identified for the simulated cases in the years 1994 and 1995 for which comparisons are made using the global model which has the TKE closure and the first-order closure PBL physics. In the present work, although the models were run for five days, the results presented are mostly confined to the 72-hour

Table 1
Brief description of NCMRWF Model T-80

Model elements	Components	Schemes
Grid	Horizontal	T-80, spectral, global
	Vertical	18 sigma layers [$\sigma = 0.995, 0.981, 0.960, 0.920, 0.856, 0.777, 0.668, 0.594, 0.497, 0.425, 0.375, 0.325, 0.275, 0.225, 0.175, 0.124, 0.74, 0.21$]
Dynamics	Prognostic variables	Rel. vorticity, divergence, virtual temp., log surface press, water vapour mixing ratio
	Horizontal transform	Orzag's technique
	Vertical differencing	Arakawa's energy conserving scheme
	Time differencing	Semi-implicit (divergence, surface press and virtual temp.) Explicit leap-frog (vorticity and mixing ratio)
Physics	Time filtering	Robert's method
	Horizontal diffusion	Fourth order
	Surface Fluxes	MONIN and OBUKHOV similarity
	Turbulent diffusion	K-theory
	Radiation	Short wave—LACIS and HANSEN (1974) Long wave—FELS and SCHWARZKOPF (1975)
	Deep convection	Kuo scheme modified
	Shallow convection	Tiedtke method (TIEDKE, 1983)
	Large-scale condensation	Manabe-modified
	Cloud generation	Slingo scheme (SLINGO, 1987)
	Rainfall evaporation	Kessler's scheme
Land surface processes	Pan method	
Gravity wave drag	LINDZEN (1981), PIERREHUMBERT (1996)	

NCMRWF GLOBAL DATA ASSIMILATION - FORECAST SYSTEM

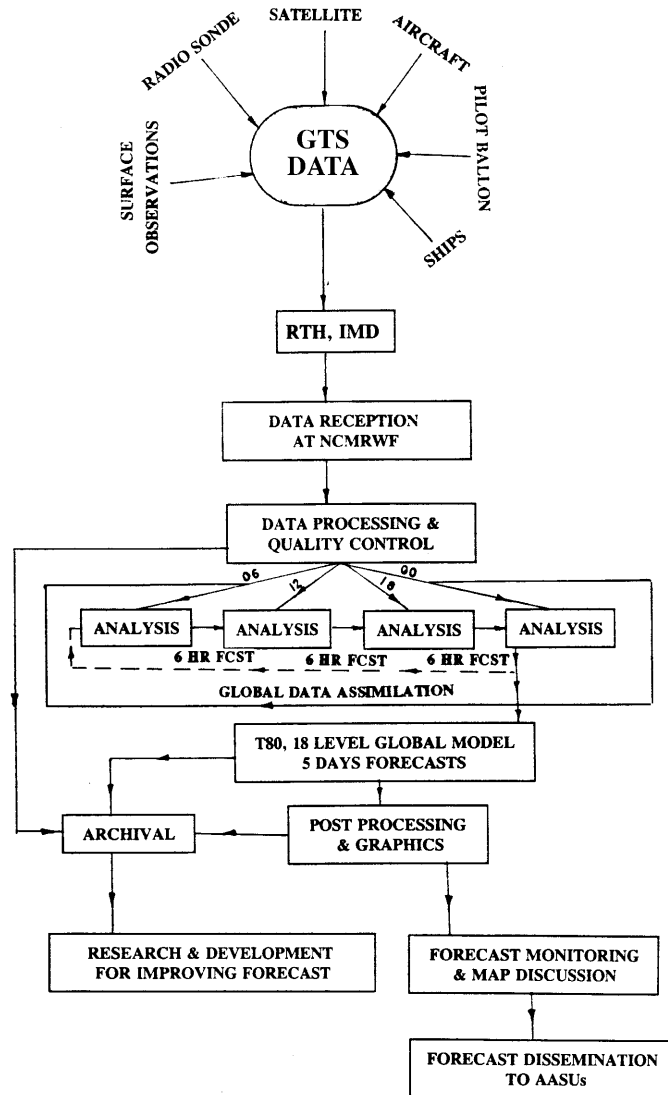


Figure 1
NCMRWF Global data assimilation and forecast system.

forecasts since the main objective is to emphasize the predictability of the monsoon systems in the medium range scale (3–5 days) with different formulations of the PBL. Two cases in 1994 and one case in 1995 were included in the current study. Although several more cases were simulated, the conclusions remain the same.

These three cases were chosen since one of the depressions originated over the Arabian Sea and remained over the ocean. The other two had formed over the Bay of Bengal and moved across land. These three cases would in general demonstrate the effectiveness of the TKE scheme in simulating tropical weather systems over both land and ocean.

3.1 Synoptic Conditions

On 5th June 1994 a depression formed over the Arabian Sea and intensified into a deep depression on 8th June and remained over the Arabian Sea. It initially moved northward and subsequently westward (the centre remaining over the ocean), giving rise to copious amounts of rainfall over the Mumbai (Bombay) region. During this phase, the onset of the monsoon had commenced over Mumbai.

During the period 29th June to 2nd July 1994, a low-pressure system had formed over northwest Bay of Bengal and traversed the country in a northwesterly direction. It dissipated over the extreme northwest parts of the country. During this period, the western and northwestern part of the country (*viz.* Rajasthan, Gujarat, Maharashtra) received ample amounts of rainfall.

A monsoon depression originated over the Bay of Bengal on 30th August 1995 at 85°E, 18°N. It made landfall on August 31, 1995 and subsequently advanced in a northwesterly direction. The depression was located over central India on 2nd September 1995. Thereafter, the system progressed in a west northwesterly direction and by 4th September it had weakened. Under the influence of this system, the eastern and western parts of the peninsula received copious amounts of rainfall. The track of this depression is shown in a later section.

In order to examine the influence of the PBL physics on the monsoon depression, two sets of numerical experiments were carried out. The model with TKE (hereafter referred to as MTKE) was run with the initial conditions of 5th and 29th June 1994 and 30th August 1995 (00 UTC), and five-day forecasts were prepared. These were then compared with the predictions from the operational model with a far simpler PBL formulation which is referred to as Model with First Order Closure (MFOC) in this paper. Both model results are verified for their merit against the observational analysis fields.

4. Description of the Schemes

The PBL parameterisation in the NCMRWF model uses the first-order closure approximation (KANAMITSU, 1989) whereby the turbulent fluxes are correlated to the mean vertical gradients through eddy diffusivities. These eddy

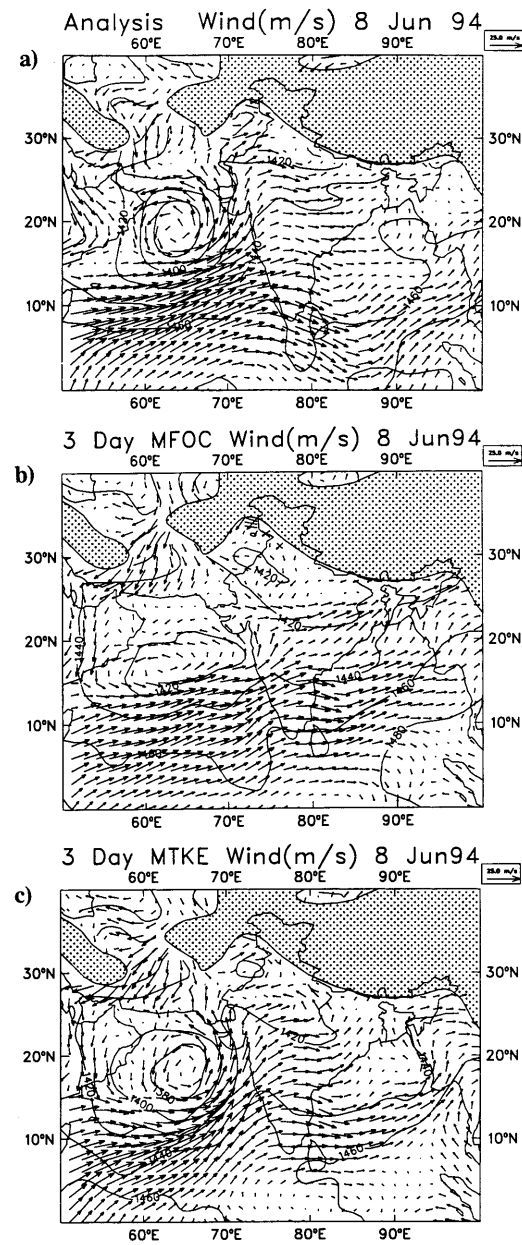


Figure 2

Geographical distribution of 850 hPa wind vectors (m s^{-1}) and geopotential heights (m) over monsoon region for 8 June, 1994. a) Verifying analysis, b) 72-hour forecast by MFOC, and c) 72-hour forecast by MTKE.

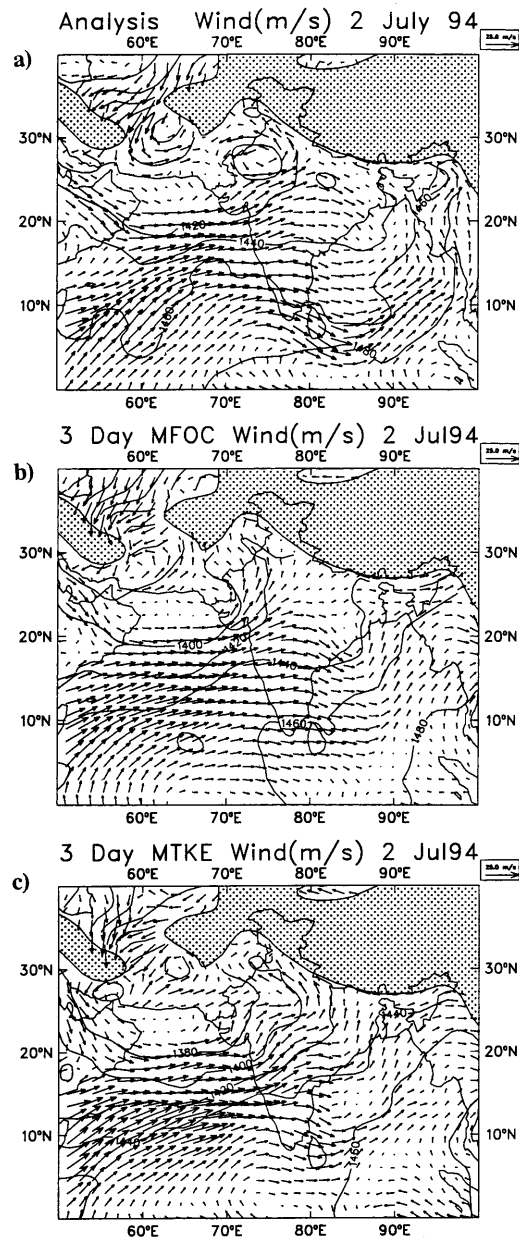


Figure 3
Same as Figure 2 but for 2 July, 1994.

diffusivities are stability dependent (through the bulk Richardson numbers) and are also functions of mixing lengths (BLACKADAR, 1962) as given below;

$K = l^2 S |dv/dz|$; where l = mixing length given by

$$1/l = 1/\kappa z = 1/250 \quad \text{where } \kappa = 0.4 \text{ (von Karman constant)}$$

S is a semi-empirical stability function related to the Richardson number R given by

$$R = \frac{g}{\Theta_v} \frac{\partial \Theta_v / \partial z}{\left| \frac{\Delta V}{\partial z} \right|^2}.$$

For stable atmosphere, i.e., $R > 0$

$$S = 1/(1 + 5R)^2 \text{ for momentum, heat and moisture}$$

For unstable atmosphere, i.e., $R < 0$

$$S = (1 + (8\sqrt{21})\sqrt{|R|} + 8|R|)/(1 + (8/\sqrt{21})\sqrt{|R|}) \quad (1a)$$

for momentum and

$$S = (1 + (12/\sqrt{87})\sqrt{|R|} + 12|R|)/(1 + (12/\sqrt{87})\sqrt{|R|}) \quad (1b)$$

for heat and moisture.

The mixing length varies as κz where κ is the von Karman constant close to the ground but approaches a value of 200 m in the mixed layer. There are several limitations in the mixing length theory (STULL, 1988), the most significant being its inability to represent the convective boundary layer realistically. In the tropics, the land surface becomes very warm during summer. As a result boundary layer becomes highly convective and the mixing length theory is inadequate. Moreover, since this theory is based on the assumptions of linear gradients, it may be valid only close to the ground. An improvement in the simplicity of first-order closure is a scheme in which the turbulent nature of the atmosphere is taken into account for the determination of the eddy diffusivity (BELJAARS *et al.*, 1987; DETERING and ETLING, 1985; KITADA, 1987; HOLT and RAMAN, 1988). It has been demonstrated by SHARAN and GOPALAKRISHNAN (1997), that in a one-dimensional model TKE closure has an edge over the other simpler closure schemes for producing the essential features of a stable boundary layer. Other studies with one-dimensional PBL models which use TKE closure over India (BASU and RAGHAVAN, 1986; RAGHAVAN and BASU, 1988) have also shown good comparison with observations. The TKE closure entails the inclusion of prognostic equations for the turbulent kinetic energy and energy dissipation rate. Here, the eddy diffusivity is determined through the turbulent kinetic energy (e) and the dissipation rate (ϵ), thus avoiding uncertainties associated

with the mixing length (LUMLEY, 1980; MARCHUK *et al.*, 1977). In the turbulent kinetic energy scheme, the diffusivity K is expressed as

$$K = C_2 e^2 / \varepsilon; \quad \text{where } C_2 = 0.90$$

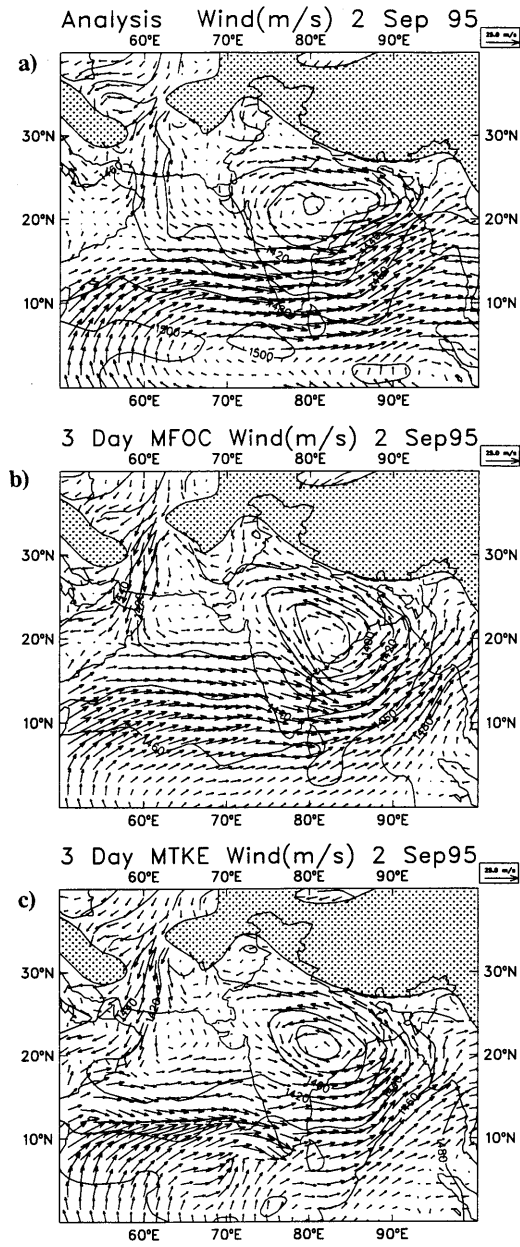


Figure 4

Same as Figure 2 but for 2 September, 1995.

and

$$e = 0.5 * (\overline{u'^2} + \overline{v'^2} + \overline{w'^2})$$

where $\overline{u'^2}$, $\overline{v'^2}$ and $\overline{w'^2}$ are the turbulence variances in the three orthogonal coordinates.

The first-order closures also arduously represent counter gradient fluxes in the upper levels of the boundary layer. The TKE closure with the correction term for counter gradient flux eliminates this problem. The TKE closure calls for solving a prognostic equation for the turbulent kinetic energy e which is given by (assuming horizontal homogeneity)

$$\partial e / \partial t = K_m \{ (\partial u / \partial z)^2 + (\partial v / \partial z)^2 \} + g / \theta \{ K_h (\partial \theta / \partial z - \gamma_{eg}) \} + c \partial / \partial z \{ K_m (\partial e / \partial z) \} - \varepsilon. \quad (2)$$

Here, in the right-hand side, the first term represents the shear production, the second buoyancy production, the third, turbulent transport and the fourth the dissipation of TKE which is determined diagnostically in the surface layer and prognostically in the remainder of the boundary layer. The prognostic equation of the dissipation of TKE is given by

$$\frac{\partial \varepsilon}{\partial t} = C_3 (\varepsilon / e) \{ -\overline{u'w'} (\partial u / \partial z) - \overline{v'w'} (\partial v / \partial z) + g / \theta (\overline{w'\theta'}) \} - C_4 (\varepsilon / e) + C_5 \{ K_m (\partial \varepsilon / \partial z) \}. \quad (3)$$

Here, the first term on the right hand side represents the generation of ε , the second term represents the destruction of ε and the third term the turbulent transport. The constants used are given as

$$C_3 = 1.44; \quad C_4 = 1.92; \quad C_5 = 0.77.$$

The TKE scheme used here, involves the inclusion of the countergradient term γ_{eg} in the temperature equation as well as in the buoyancy term of Eq. (2) which deals with the nonlocal effects. This is called the ‘‘countergradient’’ term because it acts against the local gradient for $\partial \theta / \partial z > 0$. For specific humidity, however, the nonlocal transport effect works in the same direction as the local transfer. As a result, the specific humidity does not evidence a countergradient effect. In addition, no nonlocal transport term has been derived for the wind components, and hence for simplicity we have not considered countergradient effects connected with the momentum equations. The dissipation term for TKE includes the countergradient effect in the expression of $\overline{w'\theta'}$ given by

$$\overline{w'\theta'} = -K_h (\partial \theta / \partial z - \gamma_{eg}).$$

In the present study, a constant value of $0.7 \times 10^{-3} \text{ }^\circ\text{K m}^{-1}$ is assumed for γ_{eg} .

5. Results and Discussion

Figures 2(a)–(c) show the flow pattern at 850 hPa of the verifying analysis, and 72-hour forecasts by MFOC and MTKE, respectively with the initial condition of 5th June, 1994. As seen, the analysis at 850 hPa indicates a closed circulation centered around 65°E, 18°N with a central geopotential height of 1380 m. The MFOC predicts a much weaker system which is not well defined (with a geopotential height of 1420 m). MTKE on the other hand predicts a well-defined system with a central height of 1380 m at 850 hPa centered around 67°E, 18°N. The system is very well simulated by the MTKE both in strength and location. The MTKE simulates the system better at higher altitudes as compared to MFOC (not shown).

Figures 3(a)–(c) show the flow pattern at 850 hPa of the verifying analysis, and 72-hour forecasts by MFOC and MTKE, respectively with the initial condition of 29th June, 1994. As seen in the verifying analysis, the system that had formed over the Head Bay of Bengal had shifted and on 2nd July it is seen to be positioned around 74°E, 28°N. It is clear that the simulation by MFOC does not contain the system after 72 hours, in contrast to MTKE. Although MTKE is unable to simulate a clear circulation, a well-defined trough is predicted at the observed location. In fact, MFOC could retain the system only until the first 24 hours. Another observed circulation around 62°E, 31°N is simulated well by MTKE, as compared to MFOC.

Figures 4(a)–(c) show the flow pattern at 850 hPa of the verifying analysis, and 72-hour forecasts by MFOC and MTKE, respectively with the initial condition of 30th August, 1995. During this period, the depression had repositioned from the Bay of Bengal to the central part of India, according to the analysis illustrated in Figure 4(a). The prediction of the location of the depression on this third day is better simulated by MTKE as illustrated in Figure 4(c). This predicted location with MTKE is closer to that of the verifying analysis. MTKE shows stronger winds and intense convergence over the Arabian Sea. In MFOC the depression is located closer to the coastline. However, the innermost contours of the geopotential height for 850 hPa within the system as predicted by both the models are comparable with the verifying analyses (1380 gpm). Collectively these three cases of the monsoon depressions/lows it is found that the overall performance of the model with the TKE closure (MTKE) is better than the MFOC. The general performance of these cases is almost similar. Therefore, the rest of the results presented in the paper is confined only to the 30th August, 1995 initial condition.

The analysis and day 3 forecasts (from the initial state on 30 August, 1995) with MFOC and MTKE of mean sea-level pressures are shown in Figures 5(a)–(c), respectively. As indicated by the analysis, the system is located over the central part of the country around 79°E, 21.5°N with a central pressure of 996 hPa. MFOC predicted the location of the system over the Orissa region, centered around 82.5°E, 19.5°N with a central pressure of 994 hPa. MTKE on the other hand predicts the

MEAN SEA LEVEL PRESSURE

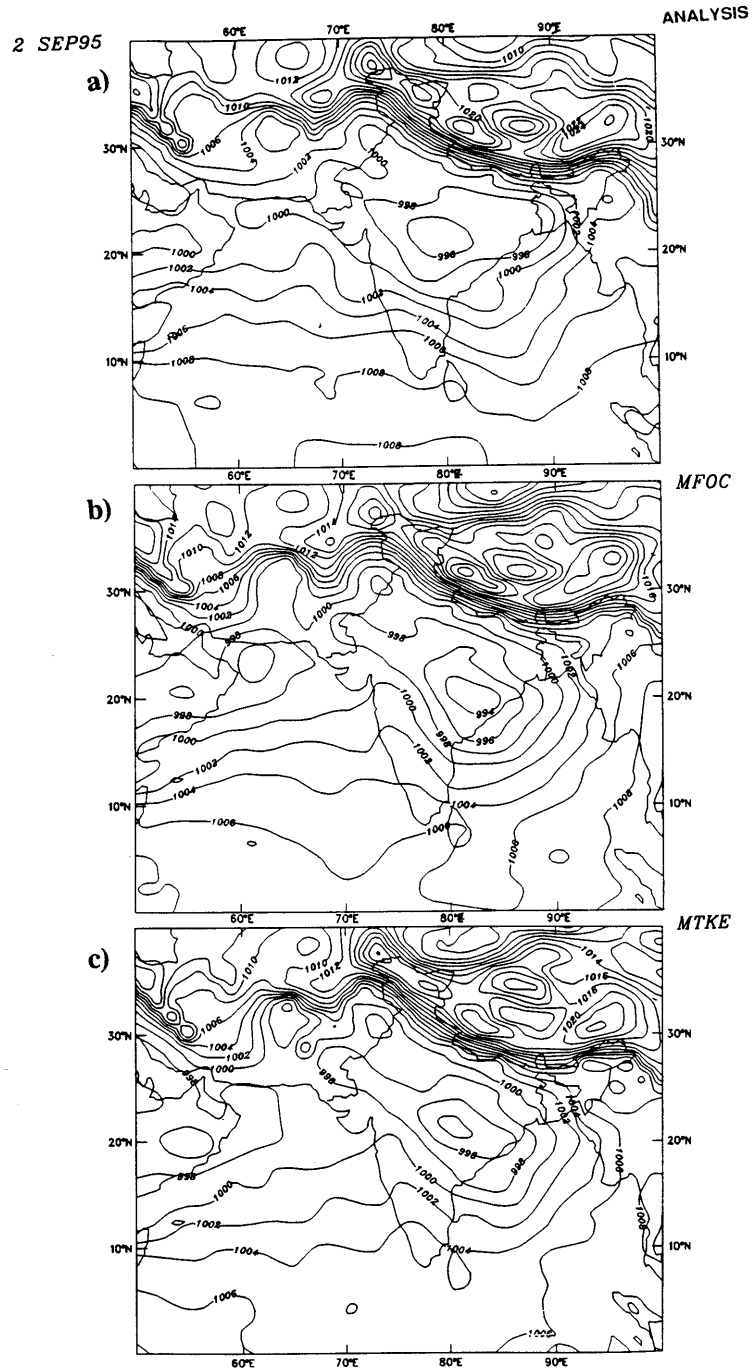


Figure 5

Geographical distribution of mean sea-level pressure (hPa) over monsoon region for 2 September, 1995.

a) Verifying analysis, b) 72-hour forecast by MFOC, and c) 72-hour forecast by MTKE.

location of the system at 81.5°E , 21°N (closer to the analysis) with a central pressure of 994 hPa. Both MFOC and MTKE predict the system to be more intense compared to the analysis. The MTKE is able to predict the location of the system closer to the observation. However, the pressure gradients on the west coast along 75°E are relatively better with MFOC.

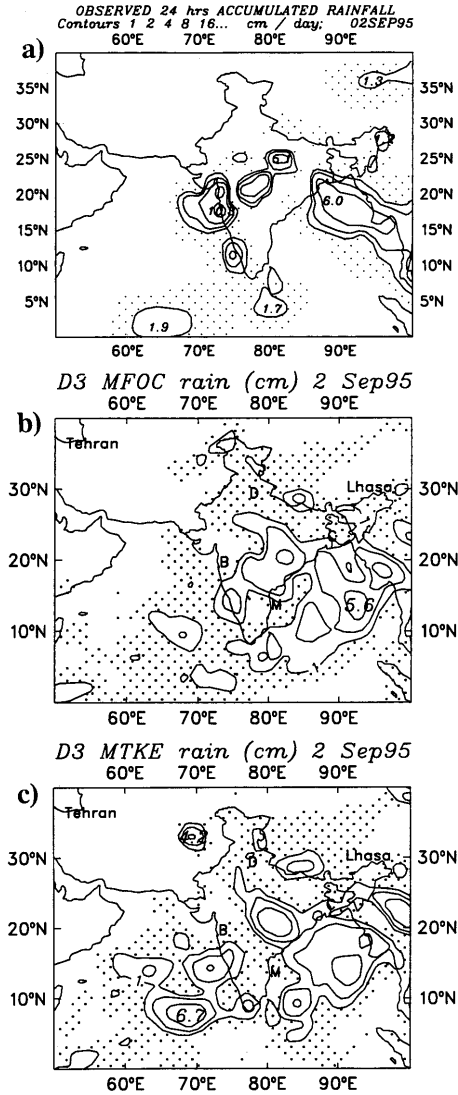


Figure 6

Geographical distribution of accumulated 48–72 hr, precipitation in cm/day for 2 Sept., 1995 over monsoon region (min. contour 1 cm) shaded areas represent precipitation < 1 cm. a) Analysed rainfall from INSAT and rain gauge, b) 72-hour forecast by MFOC, and c) 72-hour forecast by MTKE.

Rainfall analysis using rain-gauge data and quantitative precipitation estimates from INSAT IR are shown in Figure 6(a) (MITRA *et al.*, 1997). Predicted accumulated rainfall for 48–72 hr for MFOC and MTKE is given in Figures 6(b) and (c), respectively. The rainfall distribution predicted by MTKE clearly delineates two patches of rainfall along the west coast as observed, but weaker and at a slightly southern location. MFOC, on the other hand shows only one patch on the west coast and trace rainfall on the southern tip of the peninsula. Orographically induced intense precipitation over the west coast of India is not simulated adequately by both models, obviously due to the coarse resolution of the models. However, MTKE predicts somewhat larger and closer to the observed precipitation, compared to MFOC. Rainfall over the Bay of Bengal and the Arabian Sea is well simulated by both models. Rainfall simulation over central India associated with the depression is poor by both models, particularly in that the distribution relative to the depression center is not in agreement with the analysis. Further investigation is needed to simulate this feature.

Predicted 24-hour averaged surface turbulent latent heat fluxes for the MFOC and the MTKE at 72 hr are displayed in Figures 7(a) and (b), respectively. Fluxes simulated by the MTKE manifest in general higher values (by a factor of two) over land and over the oceans. There is a better distribution and stronger gradients of the fluxes for the MTKE, especially in the region of the monsoon depression. Higher values of the fluxes by MTKE are believed to be due to efficient turbulent mixing simulated by the model with the TKE closure scheme. Stronger mixing leads to larger gradients of various parameters such as wind, temperature and humidity.

Zonally averaged latitudinal variation of total evaporation (in mm) and precipitation (in mm) over 60°E–95°E at 72 hr are shown in Figures 8(a) and 8(b), respectively. In general, MTKE predicts more evaporation as compared to MFOC. For precipitation MTKE displays a peak between 20–30°N which coincides with the location of the monsoon depression. The precipitation amounts are comparable in both models. There is, however, a phase lag in the prediction of maximum rainfall by both models which could be attributed to the different locations of the systems predicted by them. The area covered by maximum precipitation is larger for MTKE as compared to MFOC.

Figures 9(a)–(c) illustrate the vertical distribution of specific humidity along the longitudes 60°E to 100°E at 21°N for the verifying analysis, and for the simulations with MFOC and MTKE, respectively. It is clearly seen that the vertical distribution of moisture by MTKE is more efficient and more realistic compared to MFOC. MFOC is seen to excessively moisten the lower atmosphere and thus is unable to transport the moisture properly to higher levels. CAPLAN *et al.* (1997) have reported a similar result in the prediction of the NCEP model with first-order closure scheme of the PBL. Though the humidity maximum has an incorrect location at surface level in MTKE, the distribution in the mid-troposphere with the hump of maximum resembled the analysis in the right zone.

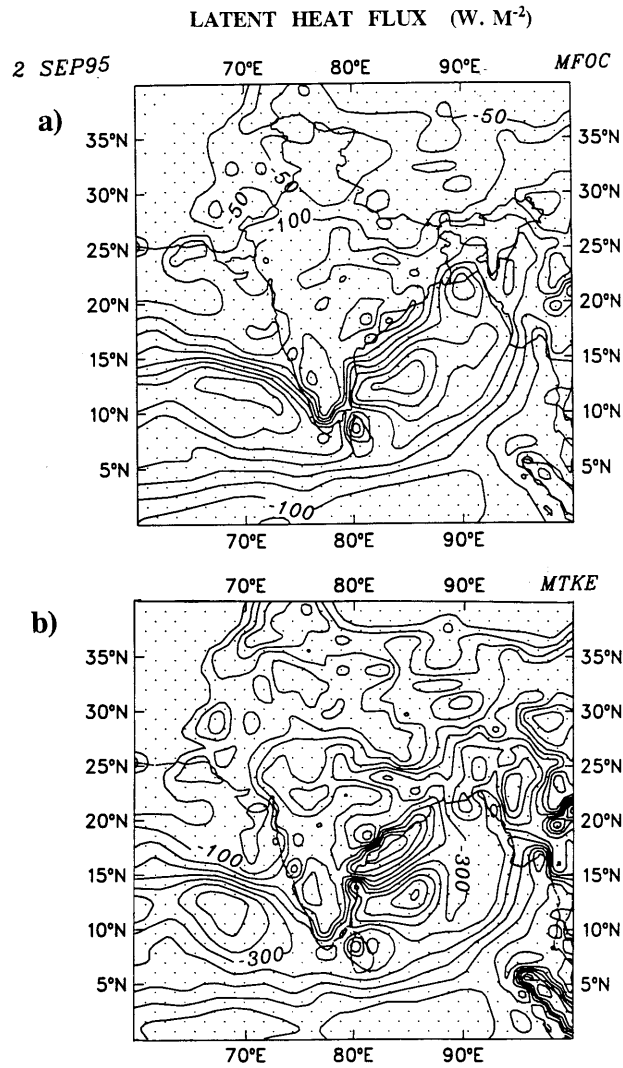


Figure 7

Distribution of 24-hour averaged surface turbulent latent heat flux (in Wm^{-2}) for 2 Sept., 1995. a) 72-hour forecast by MFOC, and b) 72-hour forecast by MTKE.

Figure 10 shows the track of the monsoon depression for a period of five days commencing on 30th August, 1995. The monsoon depression originally formed over the northern Bay of Bengal on 30th August, 1995 and advanced subsequently in a northwesterly direction as indicated by the observed track. The predicted track by MFOC indicates a northeasterly movement of the depression during the first 24 hours and a northwesterly movement in the subsequent 48 hours. The predicted movement of the depression in general is seen to be south of the observed track by

about 100 km on the third day. Rapid movement of the system is predicted on the 4th day.

The track of the MTKE simulation also indicates a small easterly movement of the depression in the first 24 hours, after which it moves in a northwesterly direction. The movement of the system is comparatively slower and is consistently closer to the observed track.

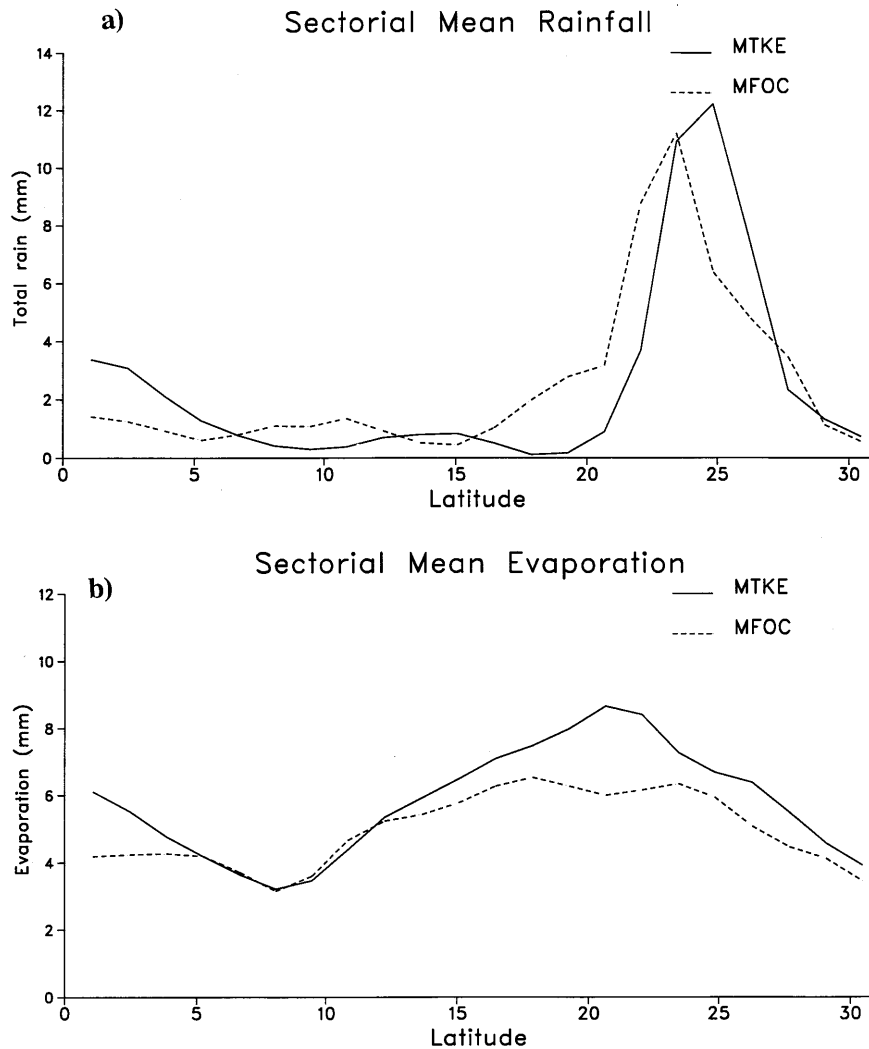


Figure 8

Latitudinal variation of sectorial averaged (from 60°E to 95°E) for 2 Sept., 1995. a) 72-hour prediction of total rain in mm by MFOC and MTKE, and b) 72-hour prediction of evaporation in mm by MFOC and MTKE.

VERTICAL SECTION HUMIDITY 21°N

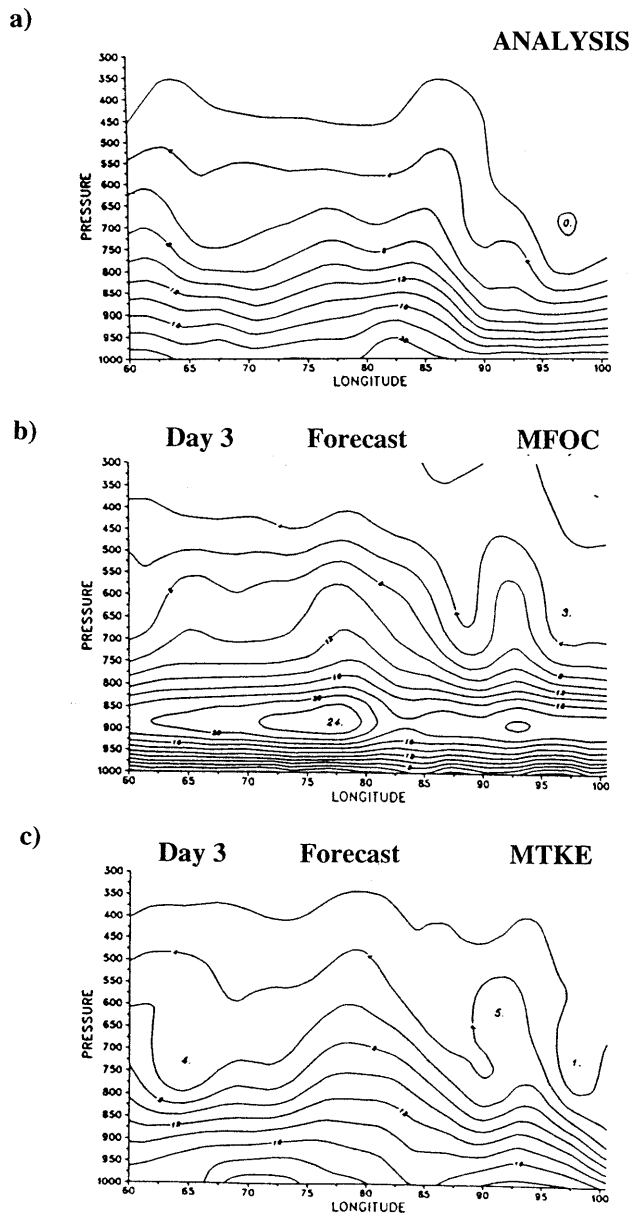


Figure 9

Vertical cross section of humidity along 60°E to 100°E at 21°N for 2 Sept., 1995. a) Verifying analysis, b) 72-hour forecast by MFOC, and c) 72-hour forecast by MTKE.

TRACKS OF DEPRESSION DURING 30th AUG – 4th SEP 1995

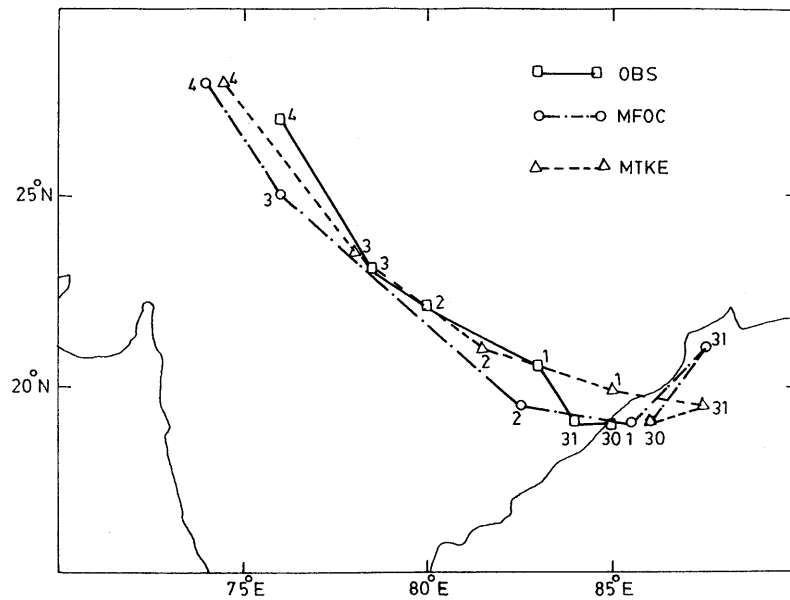


Figure 10

Track of the monsoon depression during the period 30 Aug.–4 Sept., 1995. □.....□ represent observed track, ○.....○ represent track predicted by MFOC and △.....△ represent track predicted by MTKE.

The reason for the initial eastward movement in the first 24 hours by both models could be attributed to the original mismatch of location of the analysis and the observations and spin-up problem associated with the model. Beyond 72 hours of integration the predicted track by MTKE is very close to the observations. The vector errors by the MTKE and the MFOC are exhibited in Table 2. MTKE consistently displays less vector error in all the forecast days as compared to the MFOC run.

Figures 11(a)–(d) show the characteristic features of the boundary layer structure using the TKE scheme relative to the time evolution of the TKE, boundary

Table 2

Vector error in km for 5-day forecasts of the depression (30 Aug.–4 Sept., 1995)

Forecast	MTKE	MFOC
Day 1	390	400
Day 2	210	290
Day 3	180	370
Day 4	71	320
Day 5	180	224

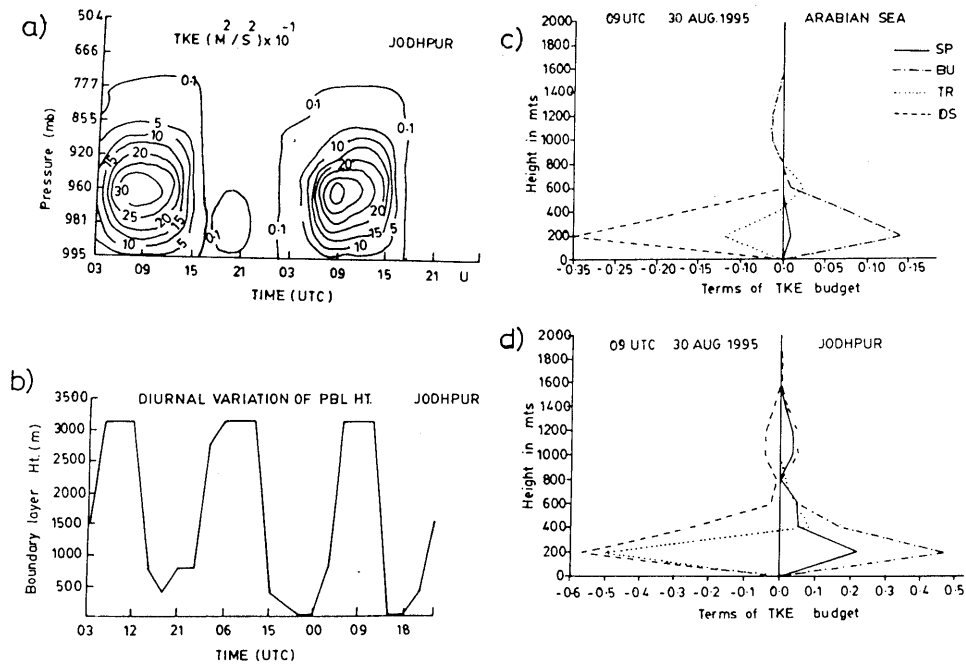


Figure 11

a) Time height cross section of TKE over Jodhpur in terms of $10^{-1} \text{ m}^2 \text{ s}^{-2}$ (IC: 00 UTC 30 August 1995). b) Time evolution of boundary layer height at Jodhpur (IC: 00 UTC 30 August 1995). c) Vertical variation of TKE Budget terms in $10^{-3} \text{ m}^2 \text{ s}^{-3}$ over Arabian Sea at 09 UTC 30 August, 1995 and d) vertical variation of TKE Budget terms in $10^{-3} \text{ m}^2 \text{ s}^{-3}$ over Jodhpur at 09 UTC 30 August, 1995. SP—Shear production; BU—Buoyancy production; TR—Transport; DS—Dissipation.

layer height, and the budgets of TKE at two different locations with an initial condition of 30 August, 1995. Since MFOC employs a simple first-order closure scheme, it is not possible to obtain similar features from the MFOC for comparison. As seen from Figure 11(a), the maximum value of TKE occurs around 350 m at Jodhpur (26.18°N , 73.04°E) at 09 UTC (1430 hrs local time), i.e., in the afternoon when the surface heating is maximum and when the mechanical generation of turbulence and buoyancy reinforce each other. During the evening TKE decreases when the dissipation and other losses exceed the production of turbulence. Similar features are observed for Wangara data as shown by STULL (1988). The maximum value of TKE is seen to be around $0.3 \text{ m}^2/\text{s}^2$. Figure 11(b) shows the diurnal variation of boundary layer height which indicates a maximum of about 3 km and a minimum of about 100 m. As mentioned earlier, and shown in Table 1, the model levels are quite discrete as a result of which the diurnal variation displays an uneven structure. Nonetheless the sequence of maximum and minimum height agrees well with the TKE activity. It is clearly seen that the time of occurrence of maximum boundary layer height (09 UTC) corresponds to the time of occurrence

of maximum TKE which is quite realistic. Figures 11(c) and (d) show the budget terms of the TKE valid for 09 UTC of 30 August, 1995 over the Arabian Sea and Jodhpur, respectively. The vertical variation of different terms indicate realistic patterns and agree well with the results of RAO *et al.* (1996) for similar conditions. It is seen that for both the locations viz. over Jodhpur and the Arabian Sea, both the production and buoyancy terms are positive, indicating convective activities during daytime. The magnitudes over the Arabian Sea are, however, considerably less in comparison to Jodhpur since, the oceanic surfaces do not experience prolonged diurnal cycles. The turbulent transport term neither creates nor destroys TKE, it just redistributes TKE from one location in the boundary layer to another. As regards the dissipation term, the rate of dissipation is highest at the level at which TKE production is the largest, i.e., near the surface. These features are observed both over the Arabian Sea and Jodhpur. The overall values over the Arabian Sea are less compared to Jodhpur for the reasons stated.

6. Conclusions

The present study discusses the effects of employing two different boundary layer schemes in a global model in the prediction of three monsoon depression systems over India during 1994 and 1995. Of these three systems, two had formed over the Arabian Sea and the Head Bay of Bengal during 1994 and one during 1995 formed over the Bay of Bengal and moved subsequently in a northwesterly direction. The global model with different PBL parameterization schemes was used to simulate the structure and the track of a monsoon depression for five days with the initial condition of 30-th August, 1995. Simulation of the other two systems for 1994 was obtained with the initial conditions of 5th June and 29th June, 1994.

The model with the TKE closure simulated the monsoon depression better, both in strength as well as in its track for the 1995 monsoon depression. This trend existed for the entire five days. The reason for a better performance by the MTKE is attributed to more realistic representation of the PBL by the TKE closure and its capacity to produce more efficient turbulent transport mechanisms, as was evident from the moisture distribution in the vertical. This results in higher values of surface fluxes that help to maintain the weather systems. For the first 72 hours it was observed that the MTKE simulations were superior to the MFOC. The rainfall distribution was also better simulated by the MTKE as compared to the MFOC.

For the case study of 1994, involving a monsoon depression over the Arabian Sea, the MTKE could simulate the location as well as the strength of the system very well as compared to the MFOC, which could not retain the strength or the location. The other system which formed during 1994 over the Head Bay of Bengal and advanced over land in the northwesterly direction was also reproduced well by the MTKE compared to the MFOC. The most important aspect of the simulation

was that it could retain the system well for 72 hours whereas the MFOC was unable to retain it beyond 24 hours. With a better prediction of the depression, simulation of other features such as Somali jet were good.

In the monsoon, the semi-permanent features such as heat low, monsoon trough, Somali jet over the Arabian Sea and other low-level processes are influenced and sustained by the boundary layer processes. The case studies presented in this paper clearly indicate the effectiveness of the well simulated PBL processes in the prediction of weather systems over land as well as over the ocean. In addition, various characteristic features obtained by MTKE exhibit a realistic boundary layer structure, simulated in terms of TKE evolution, boundary layer height and the different budget terms in the TKE equation.

Acknowledgement

The authors would like to acknowledge the NCRMWF for providing necessary support during this work. The authors express appreciation to Dr. Kiran Alapathy, North Carolina State University, U.S.A. for his assistance. This work was accomplished under the UNDP consultancy program. Part of the research was funded by the US Naval Research Laboratory. The authors also appreciately acknowledge the assistance provided by Mr. Narendra Sharma and Hari Warrior in reproducing the manuscript.

REFERENCES

- ANTHES, R. A. (1977), *A Cumulus Parameterization Scheme Utilizing a One-dimensional Cloud Model*, *Mond. Wea. Rev.* 105, 270–286.
- ASNANI, G. C., *Tropical Meteorology*, Vols. I and II (G. C. Asnani, Pune, India 1993) 1202 pp.
- BASU, S., and RAGHAVAN, N. (1986), *Prediction of Inversion Strengths and Heights from a 1-D Nocturnal Boundary Layer Model*, *Boundary-Layer Meteorol.* 35, 193–204.
- BELJAARS, A. C. M., WALMSLEY, J. L., and TAYLOR, P. A. (1987), *A Mixed Spectral Finite Difference Model for Neutrally Stratified Boundary Layer Flow over Roughness Changes and Topography*, *Boundary-Layer Meteorol.* 38, 273–303.
- BLACKADAR, A. K. (1962), *The Vertical Distribution of Wind and Turbulence in a Neutral Atmosphere*, *J. Geophys. Res.* 67, 3095–3102.
- CAPLAN, P., DERBER, J., GEMMILL, W., HONG, S. Y., PAN, H. L., and PARRISH, D. (1997), *Changes to the 1995 NCEP Operational Medium-range Forecast Model Analysis-forecast System*, *Weather and Forecasting* 12, 581–594.
- DEARDORFF, J. W. (1972), *Parameterisation of the Planetary Boundary Layer for Use in General Circulation Models*, *Mon. Wea. Rev.* 100, 93–106.
- DETERING, H. W., and ETLING, D. (1985), *Application of the E-turbulence Closure Model to the Atmospheric Boundary Layer*, *Boundary-Layer Meteorol.* 33, 113–133.
- FELLS and SCHWARZKOPF (1975), *The Simplified Exchange Approximation: A New Method for Radiative Transfer Calculations*, *J. Atmos. Sci.* 32, 1475–1488.
- HOLT, T., and RAMAN, S. (1988), *A Review and Comparative Evaluation of Multi-level Boundary Layer Parameterizations for First-order and Turbulent Kinetic Energy Closure Schemes*, *Rev. Geophys.* 26, 761–780.

- KITADA, T. (1987), *Turbulence Transport of a Sea Breeze Front and its Implication in Air Pollution Transport-application of k - ϵ Turbulence Model*, *Boundary-Layer Meteorol.* 41, 217–239.
- KANAMITSU, M. (1989), *Description of the NMC Global Data Assimilation and Forecast System*, *Weather and Forecasting* 4, 335–342.
- LACIS, A. A., and HANSEN, J. E. (1974), *A Parameterization for the Absorption of Solar Radiation in the Earth's Atmosphere*, *J. Atmos. Sci.* 31, 118–133.
- LINDZEN, R. S. (1981), *Turbulence and Stress Due to Gravity Wave and Tidal Breakdown*, *J. Geophys. Res.* 86, 9707–9714.
- LUMLEY, J. L., *Second order modelling of turbulent flows*. In *Prediction Methods for Turbulent Flows* (ed. W. Kollmann) (Hemisphere, London 1980) pp. 1–31.
- MARCHUK, G. I., KOCHERGIN, V. P., KLINOK, V. I., and SUKHORUKOR, V. A. (1977), *On the Dynamics of the Ocean Mixed Layer*, *J. Phys. Ocean.* 7, 865–875.
- MITRA, A. K., BOHRA, A. K., and RAJAN, D. (1997), *Daily Rainfall Analysis for Indian Summer Monsoon Region*, *Int. J. Climatology* 17, 1083–1092.
- MOHANTY, U. C. (1994), *Tropical Cyclone in the Bay of Bengal and Deterministic Method for Prediction of their Trajectories*, *Sadhana, Academy Proc. in Eng. Sciences* 19, 567–582.
- MONIN, A. S., and OBUKHOV, A. M. (1954), *Basic Laws of Turbulent Mixing in the Atmosphere near the Ground*, *Tr. Akad. Nauk., SSSR Geophys. Inst.* 24 (151), 1963–1987.
- PANT, M. C. (1993), *Some Characteristic Features of Low-level Southwest Monsoon Flow over the Arabian Sea*, Ph.D. Thesis.
- PARRISH, D. F., and DERBER, J. C. (1992), *The NMC's Spectral Statistical Interpolation Analysis System*, *Mon. Wea. Rev.* 120, 1747–1763.
- PIERREHUMBERT, R. T. (1986), *An Essay on the Parameterisation of Orographic Gravity Observation, Theory and Modelling of Orographic Effects*, ECMWF, Reading, U.K., pp. 251–282.
- RAGHAVAN, N., and BASU, S. (1988), *Prediction of Wind Speed, Direction and Diffusivity under Neutral Conditions for Tall Stacks*, *J. Appl. Meteorol.* 24A, 801–810.
- RAMAN, S., MOHANTY, U. C., REDDY, N. C., ALAPATY, K. A., and MADALA, R. V. (1998), *Numerical Simulation of the Sensitivity of Summer Monsoon Circulation and Rainfall over India to Land Surface Process*, *Pure appl. geophys.* 152, 781–809.
- RAO, G. V., and AKSKAL, A. (1994), *Characteristics of Convection over the Arabian Sea During a Period of Monsoon Onset*, *Atmospheric Res.* 33, 235–258.
- RAO, Y. P. (1976), *Southwest Monsoon. Meteorological Monograph*, *Synoptic Meteorology* No. 1/1976. Indian Meteorological Department, India, pp. 1–367.
- RAO, KUSUMA G., LYKOSOV, V. N., PRABHU, A., SRIDHAR, S., and TONKACHEYEV, E. (1996), *The Mean and Turbulence Structure Simulation of the Monsoon Trough Boundary Layer Using a One-dimensional Model with e - l and e - ϵ Closures*, *Proc. Indian Acad. Sci.* 105, 227–260.
- SHARAN, M., and GOPALAKRISHNAN, S. G. (1997), *Comparative Evaluation of Eddy Exchange Coefficients for Strong and Weak Wind Stable Boundary Layer Modelling*, *J. Appl. Meteor.* 36, 545–559.
- SLINGO, J. M. (1987), *The Development and Verification of a Cloud Prediction Scheme for the ECMWF Model*, *Quart. J. Roy. Met. Soc.* 115, 899–926.
- STULL, R. B., *An Introduction to Boundary Layer Meteorology* (Kluwer Academic Publishers 1988) 666 pp.
- TIEDKE, M. (1983), *The Sensitivity of the Time-mean Large-scale Flow to Cumulus Convection in the ECMWF Model*, *Workshop on Convection in Large-scale Numerical Models*, ECMWF, 297–316.

(Received March 19, 1997, accepted January 7, 1999)